Rev.Adv.Mater.Sci. 10 (2005) 483-489

GENERATION OF NANOCRACKS AT GRAIN BOUNDARY DISCLINATIONS IN NANOCOMPOSITE MATERIALS

M.Yu. Gutkin, I.A. Ovid'ko and N.V. Skiba

Institute of Problems of Mechanical Engineering, Russian Academy of Sciences, Bolshoj 61, Vas. Ostrov, St. Petersburg 199178, Russia

Received: September 15, 2005

Abstract. A theoretical model is proposed which describes the generation of nanocracks at grain boundary disclinations in a nanocomposite material. The equilibrium (critical) length of the nanocrack is calculated and studied in dependence of the system parameters. It is shown that the nanocrack can change its direction at the nanoinclusion/matrix interface or propagates straight into the bulk of the nanoinclusion. The probability of nanocrack generation increases near the nanoinclusions with negative (compressive) dilatation eigenstrain. The decrease in size of a nanoinclusion diminishes the probability of nanocrack growth along the interface, if the eigenstrain is negative, and increases this probability, if the eigenstrain is positive (tensile).

1. INTRODUCTION

It is well known that strength and hardness of nanocrystalline and nanocomposite materials exceed those of their coarse-grained counterparts [1-6]. However, these materials often demonstrate brittle behavior at low and room temperatures, which limits their practical application. Investigation of the failure processes in nanocrystalline and nanocomposite materials thus seems to be very important.

As was reported by many authors (see,e. g., [2, 5, 7-11]), the mechanisms of intercrystaline fracture dominate in fine-grained nanocrystalline and nanocomposite materials. Therefore, the most probable sites for crack generation must be the defects and stress concentrators located at grain boundaries (GBs). GBs in such materials often have non-equilibrium structure which manifests itself in jumps of the misorientation angle across the GBs. The misorientation jumps are effectively described in terms of GB disclinations [6, 12, 13] which are powerful sources of elastic stresses and therefore favorable sites for crack embryo nucleation. Nowadays there are a number of theoretical models which consider the heterogeneous crack generation at superdislocations [14, 15], dislocation pile-ups [14], wedge disclination loop [16], individual straight wedge disclinations [17-19], their dipoles [20] and more complicated arrangements of wedge disclinations [17, 21].

Nanocomposite materials commonly consist of a micro- or nanocrystalline matrix and nanoscopic inclusions (nanoinclusions). Due to differences in crystalline structure and physical properties of the matrix and nanoinclusions, there exist residual elastic (misfit) stresses in such materials. The misfit stresses may stimulate or hamper the propagation

Corresponding author: gutkin@def.ipme.ru

of the micro- or nanocracks generated in the vicinity of nanoinclusions. As a result, the equilibrium (critical) size of a growing crack must depend on characteristic lengths of the nanocomposite, which are the matrix grain size, nanoinclusion sizes, and spacing between the nanoinclusions. An example of theoretical examination of microcrack generation at the phase boundaries between a matrix and a mesoscopic inclusion is given in Ref. 22. When a nanocomposite material contains GB disclinations, one should take into account the effect of both the nanoinclusion and disclination stress fields on nanocrack nucleation and further propagation.

The main aim of the present paper is to develop a theoretical model describing the generation and propagation of a nanocrack in the sum stress field of a dipole of wedge GB disclinations and a misfitting nanoinclusion.

2. MODEL

Consider a nanocrack of the length R_1 which is generated at a negative partial wedge disclination with the strength $-\omega$ belonging to a two-axes dipole of GB disclinations with the arm L (Fig. 1). Let γ_1 be the specific surface energy characterizing the nanocrack borders. It is assumed that the nanocrack propagates along the GB AO and achieves an interphase boundary separating a nanoinclusion from the matrix. The disclination dipole is a low-energy self-screened defect configuration which is directly observed in severely deformed solids (e. g., see Refs. 12, 13, 23) and often used in theoretical modeling of various GB phenomena (e. g., see Refs. 6, 13, 24-32). The nanoinclusion is modeled as a long elastically isotropic parallelepiped with a cross section $2a\times2b$ in an infinite elastically isotropic solid. Both the shear modulus G and Poisson ratio ν are supposed to be the same for the matrix and nanoinclusion. The nanoinclusion domain is characterized by a uniform dilatational eigenstrain ε^* caused by the differences in the crystalline lattice parameters and coefficients of thermal extension of the matrix and nanoinclusion.

After the nanocrack has achieved the nanoinclusion boundary, it is assumed to propagate further by the distance R_2. In the framework of the model, the nanocrack may propagate either into the bulk or along the boundary of the nanoinclusion. In the first case, the intracrystallite crack borders OB are both characterized by a specific surface energy γ_2, while in the second case, the interface crack borders OC are supposed to have approximately

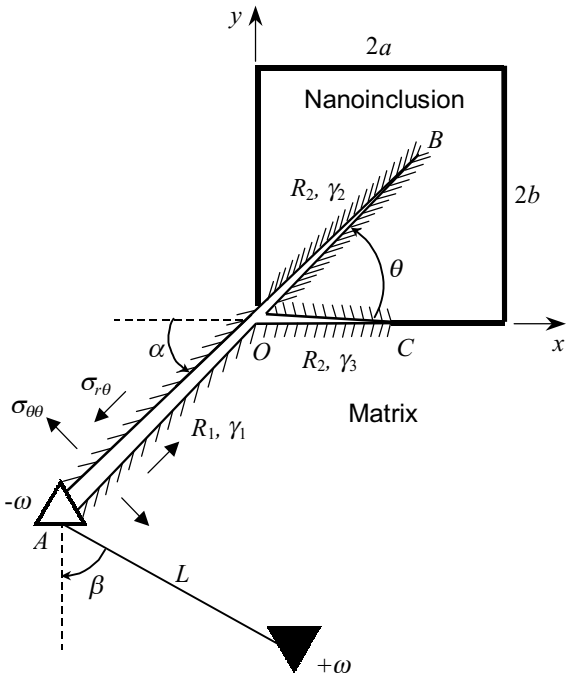

Fig. 1. Generation of nanocrack in the stress field created by both disclination dipole and nanoinclusion.

the same specific surface energy γ_3 (Fig. 1). The azimuthal angle θ determines a deviation of the nanocrack from its initial plane. Below we examine the most probable way of the nanocrack propagation inside the nanoinclusion or along the matrix/nanoinclusion interface.

At the first stage AO of its propagation, the nanocrack opens under action of the normal, $\sigma^d_{\theta\theta}(r,\theta=\pi+\alpha)$ and $\sigma^i_{\theta\theta}(r,\theta=\pi+\alpha)$, and shear, $\sigma^d_{r\theta}(r,\theta=\pi+\alpha)$ and $\sigma^i_{r\theta}(r,\theta=\pi+\alpha)$, components of the disclination dipole ($\sigma^d_{i\theta}$) and nanoinclusion ($\sigma^i_{i\theta}$) stress fields. At the next stages, OB or OC, the nanocrack also grows in the field of normal, $\sigma^d_{\theta\theta}(r,\theta)$ and $\sigma^i_{\theta\theta}(r,\theta)$, and shear, $\sigma^d_{r\theta}(r,\theta)$ and $\sigma^i_{r\theta}(r,\theta)$, stresses of the dipole and nanoinclusion. All of the stress components are written in the cylindrical coordinate system (r,θ,z) with its origin at the point O (Fig. 1). To calculate these components, we use a rectangular coordinate system (x,y,z) and the well-known nonvanishing stress components of the disclination dipole [13]

$$\sigma_{xx}^{d} = D\omega\left(\frac{(y+y_0+y_1)^2}{(x+x_0+x_1)^2+(y+y_0+y_1)^2} - \frac{(y+y_1)^2}{(x+x_1)^2+(y+y_1)^2} - \frac{1}{2}\ln\frac{(x+x_1)^2+(y+y_1)^2}{(x+x_0+x_1)^2+(y+y_0+y_1)^2}\right), \quad (1)$$

$$\sigma_{yy}^{d} = D\omega\left(\frac{(x+x_0+x_1)^2}{(x+x_0+x_1)^2+(y+y_0+y_1)^2} - \frac{(x+x_1)^2}{(x+x_1)^2+(y+y_1)^2} - \frac{1}{2}\ln\frac{(x+x_1)^2+(y+y_1)^2}{(x+x_0+x_1)^2+(y+y_0+y_1)^2}\right), \quad (2)$$

$$\sigma_{xy}^{d} = D\omega\left(-\frac{(x+x_0+x_1)(y+y_0+y_1)}{(x+x_0+x_1)^2+(y+y_0+y_1)^2} + \frac{(x+x_1)(y+y_1)}{(x+x_1)^2+(y+y_1)^2}\right), \quad (3)$$

$$\sigma_{zz}^{d} = \nu(\sigma_{xx}^{d} + \sigma_{yy}^{d}). \quad (4)$$

where $D=G/[2\pi(1-\nu)]$, $x_0=L\sin\beta$, $y_0=L\cos\beta$ and $x_1=R_1\sin\alpha$, and nanoinclusion [33]:

$$\sigma_{xx}^{i} = 2D\varepsilon^{*}(1+\nu)\left(\arctan\frac{x-x_2+a}{y-y_2+b} - \arctan\frac{x-x_2-a}{y-y_2+b} - \arctan\frac{x-x_2+a}{y-y_2-b} + \arctan\frac{x-x_2-a}{y-y_2-b}\right), \quad (5)$$

$$\sigma_{xx}^{i} = 2D\varepsilon^{*}(1+\nu)\left(\arctan\frac{y-y_2+a}{x-x_2+b} - \arctan\frac{y-y_2-a}{x-x_2+b} - \arctan\frac{y-y_2+a}{x-x_2-b} + \arctan\frac{y-y_2-a}{x-x_2-b}\right), \quad (6)$$

$$\sigma_{xy}^{i} = D\varepsilon^{*}(1+\nu)\cdot \ln\frac{[(x-x_2-a)^2+(y-y_2+b)^2][(x-x_2+a)^2+(y-y_2-b)^2]}{[(x-x_2-a)^2+(y-y_2+b)^2][(x-x_2+a)^2+(y-y_2+b)^2]}, \quad (7)$$

$$\sigma_{zz}^{d} = \sigma_{xx}^{d} + \sigma_{yy}^{d}. \quad (8)$$

where $x_2=a(1-2k)$ and $y_2=b$. When the parameter k varies from 0 to 1, the point O (where the GB AO contacts with the nanoinclusion) shifts from left to right along the bottom boundary of the nanoinclusion (Fig. 1).

Using formulae (1)-(3), (5-7) and the coordinate transforms $x=r\cos\theta$ and $y=r\sin\theta$, we can rewrite the stress components $\sigma_{\theta\theta}^{d}(r,\theta)$, $\sigma_{\theta\theta}^{i}(r,\theta)$, $\sigma_{r\theta}^{d}(r,\theta)$, and $\sigma_{r\theta}^{i}(r,\theta)$ as follows:

$$\sigma_{\theta\theta}^{j}(r,\theta) = \sigma_{xx}^{j}\sin^2\theta + \sigma_{yy}^{j}\cos^2\theta - 2\sigma_{xy}^{j}\sin\theta\cos\theta, \quad (9)$$

$$\sigma_{r\theta}^{j}(r,\theta) = (\sigma_{yy}^{j} - \sigma_{xx}^{j})\sin\theta\cos\theta + \sigma_{xy}^{j}(\cos^2\theta - \sin^2\theta), \quad (10)$$

where $j=d,i$.

To characterize quantitatively the conditions of the nanocrack generation, let us calculate in the first approximation the equilibrium (critical) length, $R=R_1+R_2$, of the nanocrack. This may be done by means of the configurational-force method [14] which was effectively exploited earlier in works [14-17,19, 21, 22]. Following Indenbom [14], the configurational force F is defined as the strain energy released when the crack moves over a unit distance. In the case under discussion, it can be written in its general form as [14]:

$$F = \frac{\pi(1-\nu)R}{4G}\left(\overline{\sigma}_{\theta\theta}^{2} + \overline{\sigma}_{r\theta}^{2}\right), \quad (11)$$

where $\overline{\sigma}_{\theta\theta}$ and $\overline{\sigma}_{r\theta}$ are the mean weighted values of the sum stress components $\sigma_{\theta\theta}=\sigma_{\theta\theta}^{d}+\sigma_{\theta\theta}^{i}$ and $\sigma_{r\theta}=\sigma_{r\theta}^{d}+\sigma_{r\theta}^{i}$, respectively. With equations (9) and (10), these mean weighted values are determined by

$$\overline{\sigma}_{\theta\theta} = \frac{2}{\pi R}\left\{\int_0^{R_1}\sigma_{\theta\theta}(r,\theta=\pi+\alpha)\sqrt{\frac{r}{R_1-r}}dr + \int_0^{R_2}\sigma_{\theta\theta}(r,\theta)\sqrt{\frac{r}{R_2-r}}dr\right\}, \quad (12)$$

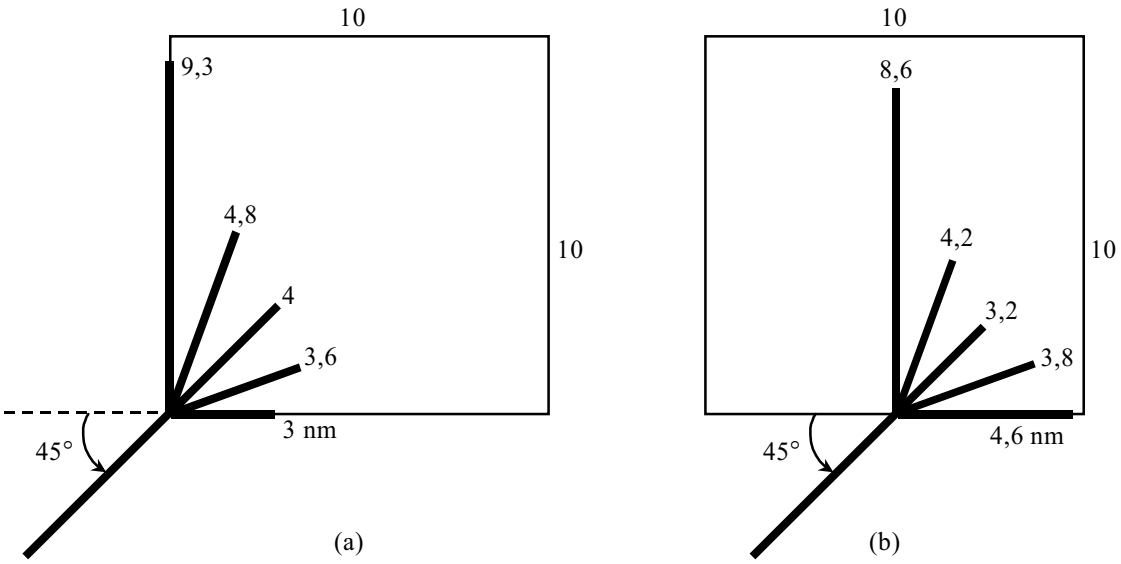

Fig. 2. Equilibrium lengths R_2 of the second segment of the nanocrack for the angles θ = 0, 20, 45, 70, and 90° (from bottom to top) at k=0 (a) and k=0.5 (b).

$$\overline{\sigma}_{r\theta} = \frac{2}{\pi R}\left\{\int_0^{R_1}\sigma_{r\theta}(r,\theta=\pi+\alpha)\sqrt{\frac{r}{R_1-r}}dr + \int_0^{R_2}\sigma_{r\theta}(r,\theta)\sqrt{\frac{r}{R_2-r}}dr\right\}. \quad (13)$$

In the first approximation in use, the equilibrium length R of the nanocrack is derived from the balance, F=2γ, between a release F of strain energy and the formation of two new nanocrack surfaces characterized by the mean surface energy density, $\gamma=(\gamma_1 R_1+\gamma_i R_2)/(R_1+R_2)$, i=2,3, per unit area. We take here the mean value for γ because the first, AO, and the second, OB or OC, segments of the curved nanocrack are characterized by different surface energies, γ_1 and γ_i, respectively. With the balance, F=2γ, and use of equation (11), we have the following equation with respect to the equilibrium length R:

$$\frac{8G\gamma}{\pi(1-\nu)R} = \overline{\sigma}_{\theta\theta}^2 + \overline{\sigma}_{r\theta}^2. \quad (14)$$

In a general case, Eq. (14) can be solved only numerically. With this equation, let us consider the equilibrium length R of the nanocrack as a function of the system parameters. It is worth noting that the equilibrium (critical) length of the nanocrack corresponds to an unstable equilibrium of the system which is characterized by its maximum total energy. Therefore, the increase of the equilibrium length R diminishes the probability of its generation under the given conditions, while the decrease of R increases this probability.

4. RESULTS AND DISCUSSION

Let us fix the length R_1 of the first segment AO of the nanocrack, and calculate the equilibrium length R_2 of the second segment (OB or OC) of the nanocrack in dependence of the angle θ. For definiteness, we assume that R_1 is equal to the arm L of the disclination dipole, and let $d\approx L\approx R_1$=30 nm. As a nanoinclusion, we take a long rod having the square cross section 10 nm $\times$ 10 nm, which is characterized by the purely dilatation eigenstrain ε^*=-0.01. Let the GB AO be inclined by the angle α=45° to the bottom boundary of the nanoinclusion, and the angle β, determining the orientation of the dipole arm, be equal to zero: β=0° (Fig. 1). For the specific surface energies, we use the following estimates: $\gamma_1\approx\gamma_3\approx 0.05GB$ and $\gamma_2\approx 0.07GB$ [34], which are typical for such FCC metals as Cu, Al, Ni, etc. Here G is the shear modulus, and B is the crystalline lattice parameter. The other parameters of the model are assumed to have the values typical for nanocrystalline materials [6]: $\omega\approx$0.1, $\nu\approx$0.3 and $B\approx$0.3 nm.

Fig. 2 shows the results of calculation of the equilibrium length R_2 of the second nanocrack segment, for different values of the angle θ, in the cases

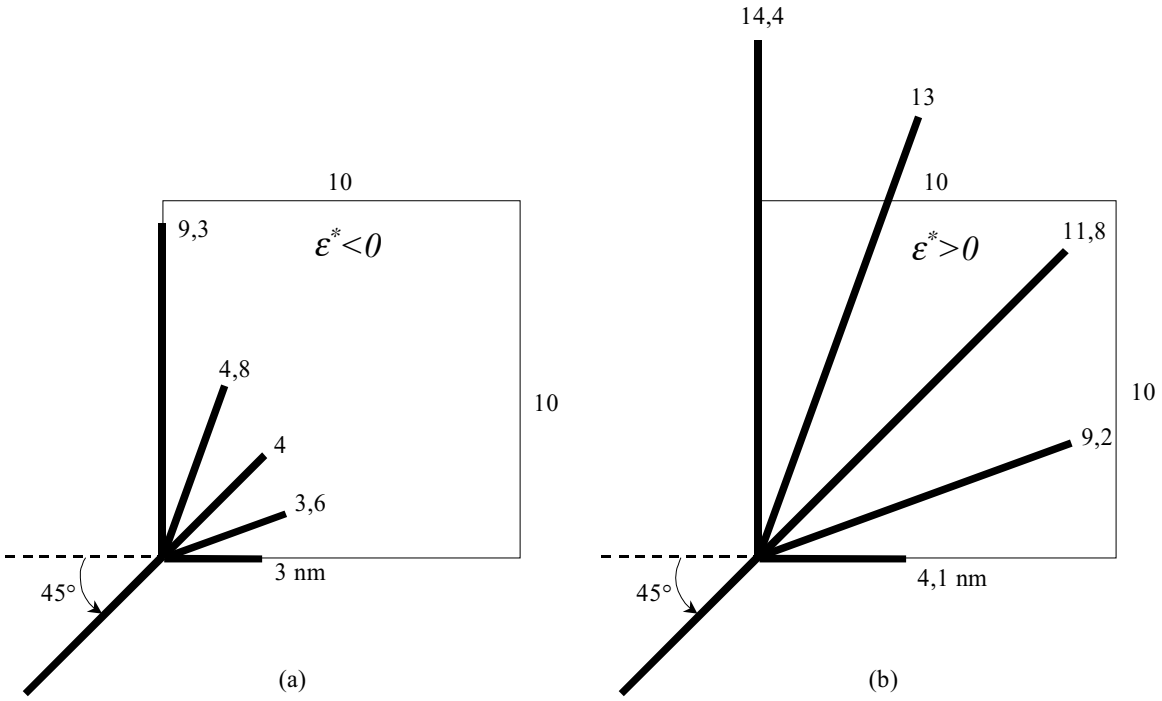

Fig. 3. Equilibrium lengths R_2 of the second segment of the nanocrack for the angles θ = 0, 20, 45, 70, and 90° (from bottom to top) and the nanoinclusion eigenstrain ε^*=-0.01 (a) and ε^*=0.01 (b).

where the GB *AO* contacts with the nanoinclusion in its corner, at *k*=0 (Fig. 2a), and in the middle of its face, at *k*=0.5 (Fig. 2b). It is seen that in the first case, the nanocrack must change its direction, and the most probable way of its propagation lies along the nanoinclusion bottom face, where the equilibrium length R_2 is minimal. As a result, the nanoinclusion exfoliates from the matrix and shears along the interface. In the second case, the nanocrack must propagate straight into the bulk of the nanoinclution, thus cleaving and shearing it. The reason of such a different behavior is the strong concentration of the nanoinclusion shear stress at the corners and along the interface. Therefore, when the GB *AO* contacts with the nanoinclusion in its corner, at *k*=0 (Fig. 2a), the nanocrack propagates mainly under the action of this stress component. In opposite, the nanoinclusion shear stress vanishes at the middle point of the interface, and the nanocrack propagation is mainly ruled by the normal (tension) stress component which is maximum at this point of the interface (Fig. 2b).

With taking as an example the situation shown in Fig. 2a, let us consider the influence of the sign of the dilatation eigenstrain ε^* upon the equilibrium length R_2. Fig. 3 demonstrates the dependence of R_2 on the angle θ for the cases of compressive ε^* (Fig. 3a) and tensile ε^* (Fig. 3b). It is seen that the nanocrack generation is more favorable near an inclusion which is characterized by a compressive eigenstrain (ε^*<0). This is so because the compressive eigenstrain produces the tensile elastic strain within the nanoinclusion. (For example, if the nanoinclusion has the coefficient of thermal extension higher than that of the matrix, then under a temperature decrease, the nanoinclusion tries to shrink stronger than the matrix and occurs to be elastically stretched.) Therefore, the elastic fields of the nanoinclusion stimulate the nanocrack to open. In the opposite case, when ε^*>0, the elastic fields of the nanoinclusion hamper the nanocrack opening, and the nanocrack propagates only under the stress field of the disclination dipole.

Let us now discuss the effect of the nanoinclusion size 2*a* on the value of the equilibrium length R_2 (i.e., the probability of the nanocrack propagation along the interface). Here we consider again the situation of a negative eigenstrain ε^*=-0.01. As shown

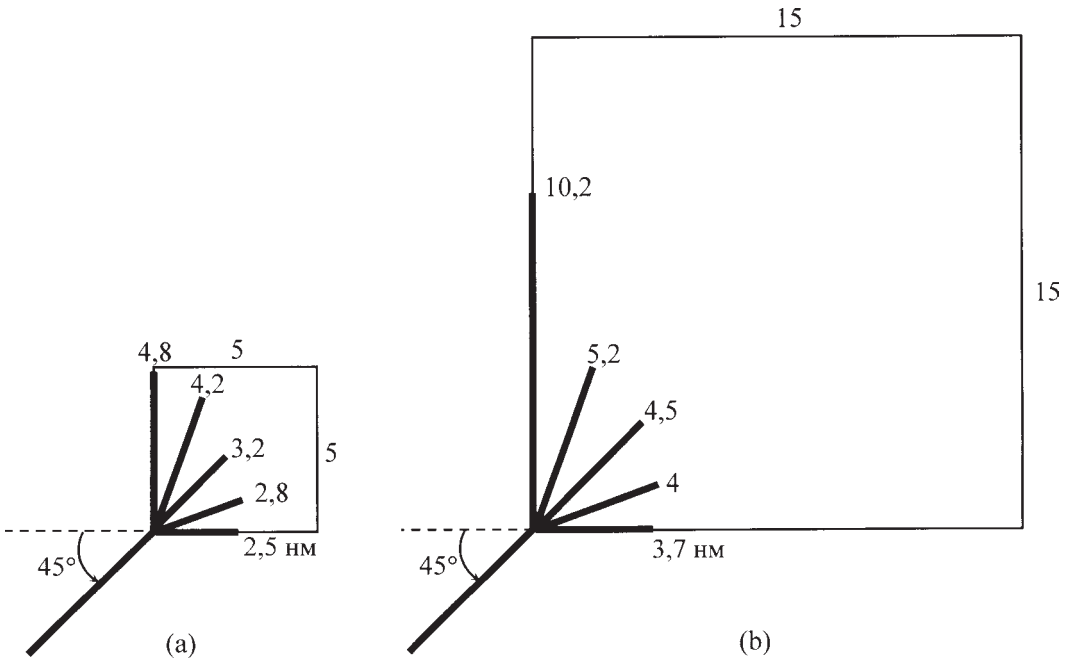

Fig. 4. Equilibrium lengths R_2 of the second segment of the nanocrack for the angles θ = 0, 20, 45, 70, and 90° (from bottom to top) and the nanoinclusion sizes 5 nm × 5 nm (a) and 15 nm × 15 nm (b)

in Fig. 4, the decrease of 2*a* from 10 to 5 nm leads to increasing R_2 (and decreasing the probability of such propagation, Fig. 4a), while the increase of 2*a* from 10 to 15 nm also decreases R_2 (and increases the probability of such propagation, Fig. 4b). These results seem to be rather natural because the values of the nanoinclusion stresses increase with its size 2*a*. As is evident, changing the sign of the eigenstrain will give just an opposite situation, when a decrease of the nanoinclusion in size will increase the probability of nanocrack propagation along the interface.

5. CONCLUDING REMARKS

Thus, in this paper a theoretical model has been elaborated which describes the generation of a nanocrack at grain boundary disclinations in a nanocomposite material. In the framework of the model, a nanocrack is nucleated at a two-axes dipole of partial wedge disclinations near a misfitting nanoinclusion having the shape of a long parallelepiped, and propagate along a grain boundary to the nanoinclusion. Depending on the point of contact with the nanoinclusion, the nanocrack can propagate along the nanoinclusion/matrix interface or into the bulk of the nanoinclusion. It is shown, that the probability of nanocrack generation increases at the nanoinclusions having negative (compressive) dilatation eigenstrain. The decrease in size of a nanoinclusion diminishes the probability of nanocrack growth along the interface, if the eigenstrain is negative, and increases this probability, if the eigenstrain is positive (tensile).

ACKNOWLEDGEMENTS.

This work was supported, in part, by the Office of US Naval Research grant N00014-05-1-0217, INTAS (grant 03-51-3779), INTAS-AIRBUS Program (grant 04-80-7339), Russian Science Support Foundation, Russian Fund of Basic Research (grant 04-01-00211), Ministry of Education and Science of Russian Federation Program *Development of Scientific Potential of High School*, Russian Academy of Sciences Program *Structural Mechanics of Materials and Construction Elements*, St.Petersburg Scientific Center, and *Dynasty* Foundation.

REFERENCES

[1] R.Z. Valiev, I.V. Alexandrov, Y.T. Zhu and T.C. Lowe // *J. Mater. Res*. **17** (2002) 5.
[2] S. Veprek and A.S. Argon // *J. Vac. Sci. Technol*. **20** (2002) 650.

[3] Y. Wang, M. Chen, F. Zhou and E. Ma // *Nature* **419** (2002) 912.
[4] X. Zhang, H. Wang, R.O. Scattergood, J. Narayan, C.C. Koch, A.V. Sergueeva and A.K. Mukherjee // *Appl. Phys. Lett*. **81** (2002) 823.
[5] K.S. Kumar, S. Suresh, M.F. Chisholm, J.A. Horton and P. Wang // *Acta Mater*. **51** (2003) 387.
[6] M.Yu. Gutkin and I.A. Ovid'ko, *Plastic Deformation in Nanocrystalline Materials* (Springer, Berlin-Heidelberg-N.Y., 2004).
[7] M. Ke, W.W. Milligan, S.A. Hackney, J.E. Carsley and E.C. Aifantis // *Mater. Res. Soc. Symp. Proc.* **308** (1993) 565.
[8] M. Ke, S.A. Hackney, W.W. Milligan and E.C. Aifantis // *Nanostruct. Maters*. **5** (1995) 689.
[9] Z. Li, S. Ramasamy, H. Hahn and R.W. Siegel // *Mater. Lett*. **6** (1998) 195.
[10] Y. Gan and B. Zhou // *Scr. Mater*. **45** (2001) 625.
[11] V.A. Pozdnyakov and A.M. Glezer // *Phys. Solid State* **47** (2005) 817.
[12] V.V. Rybin, *Large Plastic Deformations and Fracture of Metals*, (Metallurgia, Moscow, 1986) in Russian.
[13] A.E. Romanov, V.I. Vladimirov. In: *Dislocations in Solids*, ed. by F.R.N. Nabarro, Vol. 9 (North-Holland, Amsterdam, 1992) p. 191.
[14] V.L. Indenbom // *Sov. Phys. Solid State* **3** (1961) 1506.
[15] I.A. Ovid'ko and A.G. Sheinerman // *Acta Mater.* **52** (2004) 1201.
[16] V.V. Rybin and I.M. Zhukovskii // *Sov. Phys. Solid State* **20** (1978) 1056.
[17] M.Yu. Gutkin and I.A. Ovid'ko // *Phil. Mag. A* **70** (1994) 561.
[18] M.S. Wu and H. Zhou // *Intern. J. Fracture* **82** (1996) 381.
[19] M.Yu. Gutkin and I.A. Ovid'ko // *Phil. Mag. Letters* **84** (2004) 655.
[20] M.S. Wu // *Solid State Phenom*. **87** (2002) 277.
[21] M.Yu.Gutkin, K.N.Mikaelyan and I.A.Ovid'ko // *Phys. stat. sol.* (*a*) **153** (1996) 337.
[22] V.I. Vladimirov, M.Yu. Gutkin and A.E. Romanov // *Mech. Composite Mater*. **23** (1987) 313.
[23] M. Murayama, J.M. Howe, H. Hidaka and S. Takaki // *Science* **295** (2002) 2433.
[24] M.Yu. Gutkin, K.N. Mikaelyan and V.E. Verijenko // *Acta Mater*. **49** (2001) 3811.
[25] M.Yu. Gutkin, K.N. Mikaelyan, V.E. Verijenko and L.D. Thompson // *Metall. Mater. Trans. A* **33** (2002) 1351.
[26] M.Yu. Gutkin, A.L. Kolesnikova, I.A. Ovid'ko and N.V. Skiba // *Phil. Mag. Letters* **82** (2002) 651.
[27] M.Yu. Gutkin, K.N. Mikaelyan, A.E. Romanov and P. Klimanek // *Phys. stat. sol.* (*a*) **193** (2002) 35.
[28] M.Yu. Gutkin, I.A. Ovid'ko and N.V. Skiba // *Mater. Sci. Eng. A* **339** (2003) 73.
[29] M.Yu. Gutkin, I.A. Ovid'ko and N.V. Skiba // *Acta Mater*. **51** (2003) 4059.
[30] M.Yu. Gutkin, I.A. Ovid'ko and N.V. Skiba // *Phys. Solid State* **46** (2004) 2042.
[31] S.V. Bobylev, M.Yu. Gutkin and I.A. Ovid'ko // *Phys. Solid State* **46** (2004) 2053.
[32] S.V. Bobylev, M.Yu. Gutkin and I.A. Ovid'ko // *Acta Mater*. **52** (2004) 3793.
[33] M.Yu. Gutkin and I.A. Ovid'ko, *Physical Mechanics of Deformed Nanostructures. Vol. II. Nanolayered Structures* (Yanus, St. Petersburg, 2005), in Russian.
[34] D. Udler and D.N. Seidman // *Phys. Rev. B* **54** (1996) 133.